# Thermal Energy Harvesting Between the Air/Water Interface for Powering Wireless Sensor Nodes

J. Davidson[a,*], M. Collins[b] and S. Behrens[b]
[a] School of Engineering and Physical Sciences, James Cook University, Townsville, QLD, 4811, Australia
[b] CSIRO Energy Centre, 10 Murray Dwyer Circuit, Mayfield West, NSW, 2304, Australia

## ABSTRACT

Seventy percent of the Earth's surface is covered by water and all living things are dependent upon this resource. As such there are many applications for monitoring environmental data in and around aquatic environments. Wireless sensor networks are poised to revolutionise this process as the reduction in size and power consumption of electronics are opening up many new possibilities for these networks. Aquatic sensor nodes are usually battery powered, so as sensor networks increase in number and size, replacement of depleted batteries becomes time consuming, wasteful and in some cases unfeasible. Additionally, a battery that is large enough to last the life of a sensor node would dominate the overall size of the node, and thus would not be very attractive or practical. As a result, there is a clear need to explore novel alternatives to power sensor nodes/networks, as existing battery technology hinders the widespread deployment of these networks. By harvesting energy from their local environment, sensor networks can achieve much greater run-times, years not months, with potentially lower cost and weight. A potential renewable energy source in aquatic environments exists via the temperature gradient present between the water layer and ambient air. A body of water will be either a few degrees warmer or colder than the air directly above it dependant on its latitude, time of year and time of day. By incorporating a thermal energy harvesting device into the sensor node deployment which promotes the flow of heat energy across the thermal gradient, a portion of the energy flow can be converted into useable power for the sensor node. To further increase this temperature difference during the day the top section can be heated to temperatures above the ambient air temperature by absorbing the incoming sunlight. As an initial exploration into the potential of this novel power source we have developed a model of the process. By inputting environmental data, the model calculates the power which can be extracted by a thermal energy harvesting device. Initial outputs show a possibility of up to 10W/m$^2$ of power available from measured sites assuming a thermal energy harvester operating with Carnot efficiency.

**Keywords:** energy harvesting, renewable energy, solar thermal energy, thermoelectric, wireless sensor network
**Note:** Figures 1, 3, 5 & 6 are colour images and are more clearly seen online in electronic form.

## 1 INTRODUCTION

Seventy percent of the Earth's surface is covered by water. Humans and all other livings thing are dependent upon this resource. As such there are many applications for monitoring environmental data in and around water. Marine biologists, oceanographers, climatologists, environmental scientists, water quality managers and many other users currently monitor various parameters in aquatic environments to aid their understanding and decision making. Wireless sensor networks are ideal to facilitate this process.

In recent years the size and power consumption of electronics have reduced dramatically, enabling new possibilities in the field of wireless sensor networks. It is envisioned that such networks will revolutionise environmental monitoring and data acquisition with applications only limited by the user's imagination. The ability to sample data with greater spatial resolution due to decreased size and cost of the individual nodes and then to have that data available in real-time as the networks communicate results through RF transmissions gives significant benefit to users and decision makers reliant on the information being monitored. However one aspect of the sensor nodes which is lagging and hindering the widespread deployment of wireless sensor networks is a reliable power supply.

*Send correspondence to Josh Davidson: joshua.davidson@jcu.edu.au; ph. +61 7 4781 5086; www.jcu.edu.au

Active and Passive Smart Structures and Integrated Systems 2009, edited by Mehdi Ahmadian, Mehrdad N. Ghasemi-Nejhad, Proc. of SPIE Vol. 7288, 728814 · © 2009 SPIE · CCC code: 0277-786X/09/$18 · doi: 10.1117/12.815859

Currently the predominant means of powering sensor nodes is through the use of primary batteries. The amount of energy which can be provided by these batteries is limited by the amount of energy initially stored in their internal chemistries. As such the lifetime of the sensor nodes is restricted by the lifetime of the batteries powering them. To extend the operating life of the sensors it is necessary to either replace the batteries with fresh ones once they are depleted or initially install more/larger batteries thereby increasing the initial energy store. Replacing the batteries with fresh ones drastically increases the servicing costs and when the networks increase in number and size may prove unfeasible and in some cases impossible where nodes are deployed in inaccessible locations e.g. inside a concrete wall for structural health monitoring. By increasing the size of the initial energy store the physical size of the node is increased. A battery large enough to last the life of a multi-year long-term deployment would dominate the overall size of the node, thus would not be very attractive or practical. As a result, there is a clear need to explore novel alternatives to power sensor networks/nodes.

By harvesting energy from their local environment, sensor networks can overcome their power source problem achieving much greater run-times, years not months, with potentially lower cost and weight. There are numerous alternative energy harvesting options depending on the location and environment of the sensor node's deployment. Energy harvesting for wireless sensor nodes is a growing field and has been the focus of much effort from various research groups in recent years. An in depth review of the field is given in [1]. As the energy harvesting device can continually provide power from a renewable source, the node's lifetime is now limited only by the reliability of its own parts.

Sensor nodes must overcome the problem of the power supply in order to accomplish the goal of improving the environmental monitoring in and around water. A potential renewable power source exists via the temperature gradient present between the water and ambient air. A body of water will be either a few degrees warmer or colder than the air directly above it depending on it's local weather conditions, latitude, time of year and time of day. By incorporating into the sensor node deployment a thermal energy harvesting device which promotes the flow of heat energy across the thermal gradient, a portion of the energy flow can be converted into useable power for the sensor node. This concept was inspired by similar energy harvesting research exploiting the thermal gradient existing between the soil and ambient air [2,3].

This paper gives a preliminary investigation into thermal energy harvesting between the air/water interface for powering wireless sensor nodes. To increase the potential of such harvesting devices, the effect of utilizing the incoming solar radiation to heat a collector plate to a temperature above that of the ambient air is then considered.

### 1.1 Thermal Energy Harvesting

A temperature difference existing between two locations will result in a flow of heat energy from hot to cold in an attempt to develop thermal equilibrium. The heat flow can be exploited to harness useful energy. This process is governed by the laws of thermodynamics therefore its efficiency, the ratio of the useful work extracted out, $W$, to the input heat, $Q$, is constrained by the fundamental Carnot limit. The Carnot efficiency limit applies to all heat engines and generators and can be expressed in terms of the hot, $T_H$, and cold, $T_C$, temperatures as,

$$\eta = \frac{W}{Q} = \frac{T_H - T_C}{T_H} \tag{1}$$

This shows that the efficiency is very low for small to modest temperature differences. As an example, if the air was at 30 ºC and the water at 25ºC, then the maximum efficiency that the flow of heat could be harvested into useable power would be 1.6%. The Carnot efficiency limit is the maximum theoretically possible efficiency. Real world conversion devices however do not achieve efficiencies as high as this.

Hence there are many types of engines designed to extract useful work from sources of heat, examples of which range from thermally powered wrist watches to motor vehicle engines to nuclear power plants. These engines can be broadly classified into two categories; mechanical and solid state. For the application of harvesting low amounts of power for

wireless sensor nodes, from small ambient temperature gradients, solid state devices offer the best potential. This is due to their lack of moving parts which facilitates robustness and low maintenance requirements. Life testing of thermoelectric devices has shown their capability for over 100,000 hours of continuous operation [4]. They are compact and light, noiseless in operation, are highly reliable and eliminate power losses in extra conversion steps needed for mechanical engines. The dominant solid state conversion technique at present is thermoelectricity which involves the direct conversion of heat to electricity via the Seebeck effect. As such this work will assume the use of a thermoelectric (TE) device for the conversion mechanism.

# 2 POWER AVAILABLE BETWEEN WATER AND AMBIENT AIR

Figure 1(a) is a plot of the temperature of the water and the ambient air measured by the Australian Institute of Marine Science (AIMS) weather station located at Orpheus Island (Lat: 18.612808 S, Lon: 146.483094 E) every 30 minutes for a 48 hour period in late January 2008. It shows a varying temperature difference between the water and air ranging from a maximum of about 4 to 5°C in the early hours of the morning when the air is at its coldest and a minimum of 0°C when the air is at its warmest in the late afternoons. Due to the water's large thermal mass its temperature varies less than that of the air across the day. Also, it can be seen at that site for that period, in the tropics in the middle of summer, that the water temperature is greater than that of the air.

For different locations and for different times of the year, the temperature difference between the water and the air will change. At some locations the water will be at a higher temperature than that of the air while at other locations the air will be warmer than the water. For the same locations the situations may be exactly reversed 6 months later as the seasons cycle. The temperature difference will vary across the day and its magnitude and variation change throughout the year. Therefore the potential of the air/water temperature difference as a small scale renewable energy source may have a strong dependence on the location and the time of year. To get an overall picture of the potential of this resource it needs to be investigated across the globe across the full year as is depicted in Figure 1(b).

## 2.1 Global data

The map displayed in Figure 1(b) was created using data from the NCEP Reanalysis project which uses an analysis/forecast system to perform data assimilation using past data from 1948 to the present. It has global coverage using a T62 Gaussian Grid of 192 x 94 points with each set of results reported every 6 hours. The map shows the average of the absolute air/water temperature difference across the Earth's oceans. Each pixel is one of the grid points (representing approximately 190000km$^2$) from the NCEP data with the value at each pixel being calculated by firstly finding the absolute value of the air/water temperature difference for each time step. The absolute value was taken because the output power from a TE device is positive for both positive and negative temperature differences. The average of these absolute temperature differences was then calculated.

As can be seen from Figure 1(b) there is an average temperature difference of a few degrees Kelvin across all of the Earth's oceans. Some regions display a higher average than others due to local conditions ranging from dependence on latitude, shoreline proximity, incoming currents etc. An example of this is the visible effect of the Gulf Stream Current shown by the lighter areas directly east of the USA and Canada. The high values here presumably occurring due to the dominating effect of the Gulf Stream Current transporting warm water from the Equator northward into in the cold northern hemisphere winter. What can be seen from the 2 figures, which lie on opposite ends of the time and spatial scales from each other, is that the air/water temperature difference varies between about 0 and 5K. An estimate of the thermal energy available to be harvested from this resource will be conducted in the next section.

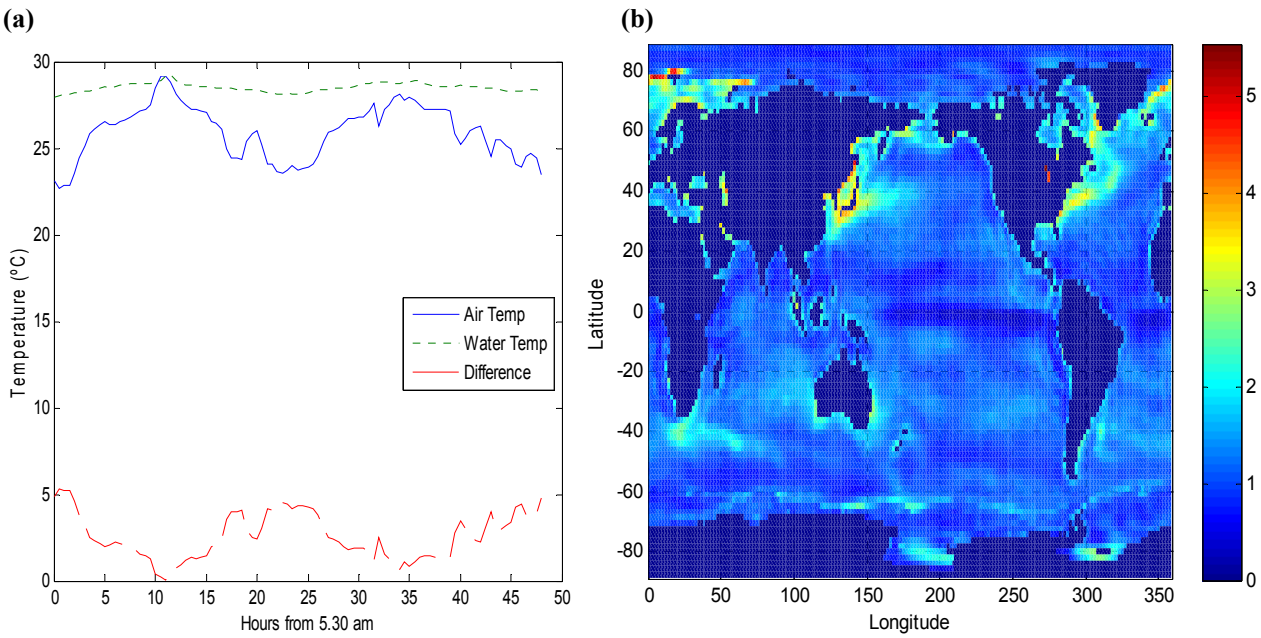


**Figure 1: (a) Air and water temperatures measured at Orpheus Island for the 48 hours following 5.30am 26/01/2009 (b) Average of Absolute Air/Water Temperature difference in degrees Kelvin for 2008**

### 2.2 Energy Harvesting Model

The process is modeled on a thermal energy harvesting device with a physical set up depicted schematically in Figure 2. The expected air/water temperature difference is only a few degrees Kelvin therefore the energy conversion will be limited by a very low Carnot efficiency. The low efficiencies of this process necessitate a large amount of heat to be transferred through a device in order for it to harvest useful amounts of work. Thus a good thermal conductor is introduced across the air/water interface to promote a generous heat flow. The airside and waterside heat exchangers are assumed to thermalise with the ambient air and water respectively. A heat pipe, consisting of a thermal conductor insulated around its outside, then acts as an efficient medium for heat transfer between the exchangers. Sandwiched in the middle of the heat pipe is a TE module which converts the flow of heat into useable power.

The configuration from Figure 2 is then modeled as follows. It is firstly assumed no temperature drop occurs in the heat pipe between the exchangers and the TE device and also that the exchangers are always in thermal equilibrium with the surrounding medium i.e. at the same temperature as that measured for the water and air. Therefore the temperature difference across the TE device is

$$\Delta T = T_a - T_w \tag{2}$$

The rate of heat transfer through the TE device due to conduction is

$$\dot{Q} = kA\frac{\Delta T}{\Delta x} = kA\frac{T_a - T_w}{\Delta x} \tag{3}$$

Where $k$ is the thermal conductivity of the TE device, $\Delta x$ is the thickness of the TE device which is set at 1cm and $A$ is its area which is 1m$^2$ so that the results can conveniently be quoted as Watts per square meter. These results can easily be scaled to different device configurations via the linear dependency of the 3 device parameters $k$, $A$ and $\Delta x$.

Currently most TE devices are comprised from the semi-conducting material Bismuth Telluride, thus its quoted thermal conductivity of 1.20 W/(m·K) [5] will be used for $k$ in the work to follow.

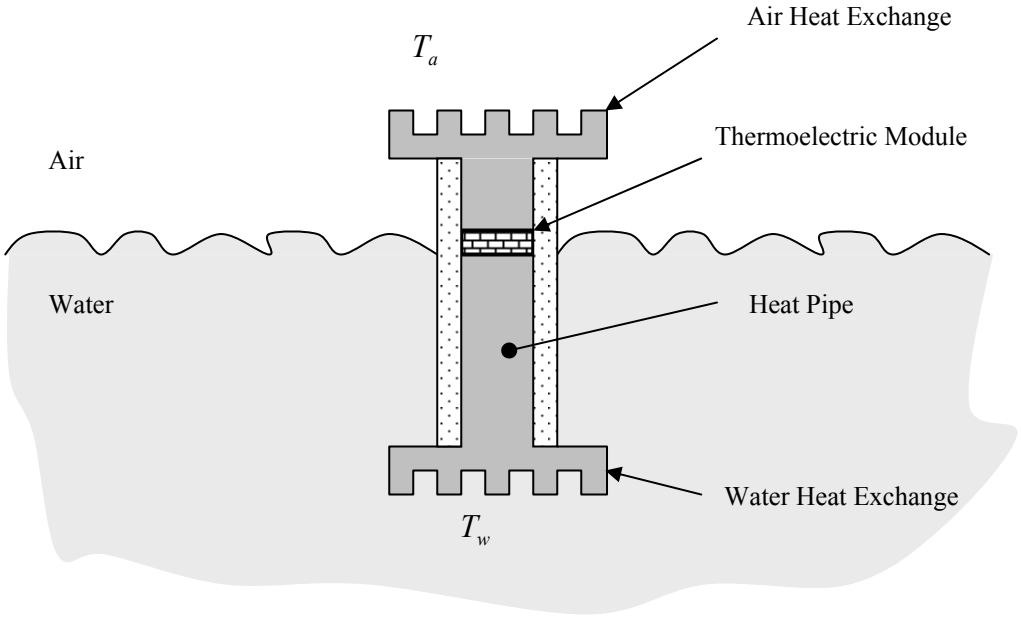


Figure 2: Thermal Energy Harvesting Device

Equation 3 gives the amount of heat flowing through the TE device per unit time. Therefore multiplying this by the Carnot efficiency will yield the maximum theoretically possible power output a thermal energy scavenging device could harvest from the heat flow. TE devices operate at efficiencies much lower than the Carnot limit but as their efficiencies vary from device to device and also are continually increasing with improving technology the Carnot efficiency is used to give an upper bound to the amount of power achievable. The results can then be multiplied by the percent of Carnot efficiency a particular TE device can actually achieve to give a more precise value.

$$Power\ Output = (Rate\ of\ Heat\ Flux)(Carnot\ Efficiency)$$
$$P_{out} = kA\frac{(T_a - T_w)}{\Delta x}\frac{(T_a - T_w)}{T_a} = kA\frac{(T_a - T_w)^2}{T_a \Delta x} \quad (4)$$

This assumes an air temperature greater than water temperature but can be corrected for the equally likely case of water temperature greater than air by replacing the $T_a$ term in the denominator by $T_w$. Applying the 2 datasets from Figure 1 to this model gives the outputs displayed in Figure 3.

Figure 3(a) shows the power output from the air/water interface at the AIMS Orpheus Island site. It has a maximum of about 11 W/m$^2$ occurring early in the morning dropping down to around zero in the late afternoons with a mean output across the two days of 3.3W/m$^2$. The fluctuation of this output will be examined further in the discussion section. From Figure 3(b) it can be seen that on average throughout the year across the globe a power output in the order of 100mW/m$^2$ is achievable from a thermal energy harvesting device. Some areas such as around Japan, the west North Atlantic and to the north of Scandinavia have values much greater than this.

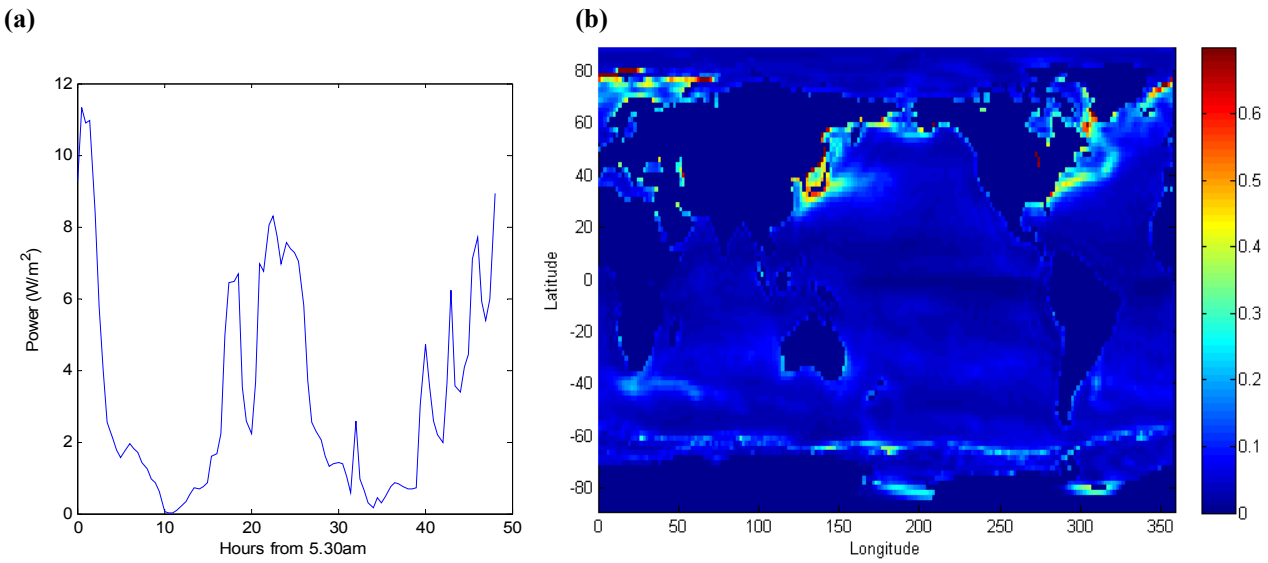


Figure 3: (a) Power output from thermal energy harvester model for the temperature inputs from Figure 1(a) , (b) Avergage power from thermal energy harvester model in W/m$^2$ for 2008

## 3 HARNESSING SOLAR INSOLATION

The previous section showed that the power output from a thermal harvesting device is proportional to the square of the temperature difference. Therefore any possible increase to this temperature difference will result in large gains to the power output. As such using the heat from the incoming solar radiation to increase the air side temperature of the TE device above the ambient air temperature will be investigated.

A black object left unshaded from the Sun will heat up as it absorbs the incoming sunlight. This motivated the design shown in Figure 4, which is similar to the original design in Figure 2 with the addition of a black solar collector plate on the top side. The plate absorbs the incoming sunlight and rises to temperatures above the ambient air. To model this we need to account for all heat transfer processes occurring on the plate. Figure 4 shows three sections to the device. There is the top section which is exposed to the atmosphere collecting the incoming solar radiation, there is the TE device section in the middle through which heat is conducted and then there is the bottom section which acts as the heat sink into the water. The bottom section is assumed to be in thermal equilibrium with the water. The size of the device used in the model is 1m$^2$ so that all values reported can conveniently be quoted per square meter (m$^2$).

The top section has 4 different heat transfer processes acting on it; the incoming solar radiation, $Q_s$, conduction down through the TE device, $Q_c$, convection from its top surface, $Q_v$,, and outgoing radiation, $Q_r$. The rates of these 4 processes can be expressed as

$$\begin{aligned} \dot{Q}_s &= \alpha A_c I \\ \dot{Q}_c &= kA_{TE}\frac{T - T_w}{\Delta x} \\ \dot{Q}_v &= hA_c\left(T - T_a\right) \\ \dot{Q}_r &= \varepsilon\sigma A_c\left(T^4 - T_s^4\right) \end{aligned} \qquad (5)$$

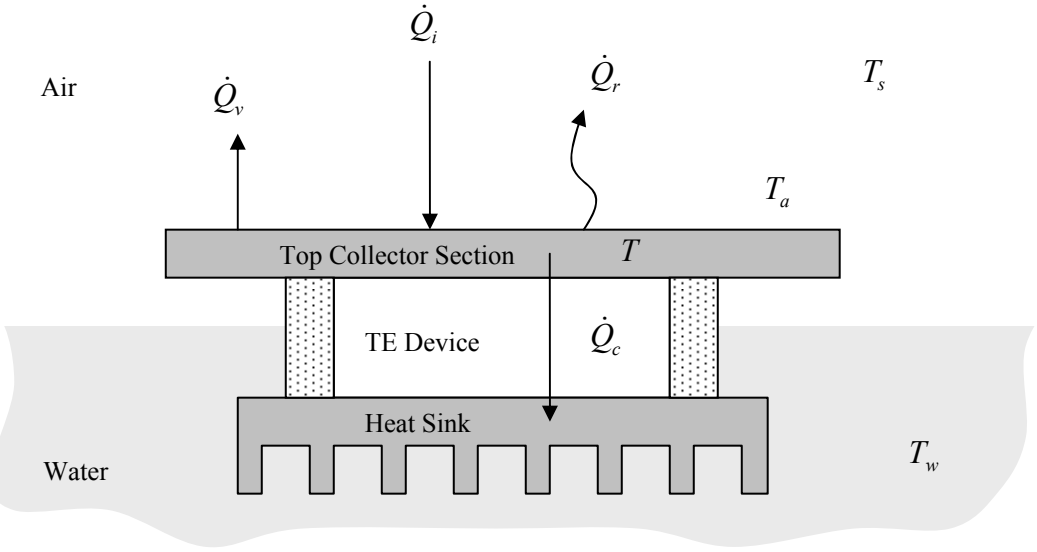


Figure 4: Physical Setup of the solar thermal concept

Where the overdot denotes time rate, $A_c$ and $A_{TE}$ the areas of the collector plate and TE device respectively, α is the absorptivity of the collector plate, $I$ the incoming solar insolation, $h$ the convection coefficient, $\varepsilon$ the emissivity of the collector plate, $\sigma$ is Stefan-Boltzmann's constant and $T$, $T_w$, $T_a$ and $T_s$ the collector, water, air and effective sky temperatures respectively. Note the minus sign before the $\dot{Q}_c$, $\dot{Q}_v$ and $\dot{Q}_r$ terms which normalises these transfer processes to remove heat from the collector when its temperature is at a higher value than its surroundings. The total rate of heat transfer to/from the top section is therefore

$$\dot{Q}_t = \dot{Q}_s - \dot{Q}_c - \dot{Q}_v - \dot{Q}_r$$
$$\dot{Q}_t = \alpha A_c I + kA_{TE}\frac{T - T_w}{\Delta x} + hA_c\left(T - T_a\right) + \varepsilon\sigma A_c\left(T^4 - T_s^4\right) \tag{6}$$

The net amount of heat energy absorbed/emitted by the top plate in a given time, $\Delta t$, is then

$$Q = \dot{Q}_t \Delta t \tag{7}$$

The heat energy flowing into/out of the collector will cause a temperature change given by

$$\Delta T = \frac{Q}{m\,c} \tag{9}$$

Where $m$ is the mass of the collector plate and $c$ is its specific heat capacity. For use in the model, a 1cm thick aluminium collector plate is used which gives an $mc$ value of 24,300 J/K.

The model runs iteratively, updating the temperature of the top section at each new iteration as

$$T_{n+1} = T_n + \Delta T \tag{10}$$

until

$$Q_t = 0 \ \ / \Delta T = 0 \tag{11}$$

i.e. the device reaches steady state. The power output can then be calculated as the rate of heat flowing through the device, $Q_c$ multiplied by the Carnot efficiency, $\eta$.

### 3.1 Optimising TE Device Area

Before the model can be used to determine available power outputs the effect of the ratio of the TE device and collector plate areas needs to be considered. Decreasing the TE device area decreases the heat flow through it and thus increases the temperature difference between the top and bottom sections. The increased temperature difference has the effect of increasing the Carnot efficiency and therefore the efficiency of energy conversion but decreasing the heat flow decreases the amount of energy available for conversion. There is an optimum TE device area which allows a good heat flow through the TE device while maintaining a high temperature difference across it.

A thorough investigation of calculating the optimum TE device area is outside the scope of this paper, however a quick approximation to the optimum was performed to give a rough indication of what TE device area to use in the present model. The model was run using the Orpheus Island data with the TE device area being incrementally varied in each successive run. The average power across the two days was calculated for each TE device area and a clear peak was found when the TE device area was about 1% of the collector area. It should be noted that this assumes the temperature does not vary across the collector plate. In reality the fraction of the collector plate directly above the TE device will be a different temperature than the plate not above the TE device due to the extra heat transfer there. This will result in thermal gradients developing across the plate's surface with conduction flowing between these regions. To account for this effect in this rough approximation the TE device area will be increased to 5% of the collector area however a more in depth 2-D model of the process needs to be implemented to choose a more accurate value.

### 3.2 Absorptivity and Emissivity

Initially the absorptivity and emissivity of the collector plate were set as equal to 0.9. This lead to power outputs marginally greater than those in Section 2 without the solar thermal collection. To improve this, the energy harvester will utilize selective absorbing materials. These materials are designed to have high absorptivity in the visible light range of the spectrum while having low emissivity in the infra-red range which is where the collector plate will be emitting most of its energy [6]. Common selective absorbing materials can have an absorptivity of 0.9 with an emissivity of 0.1, hence these values are used to obtain the results.

### 3.3 Results

The model was applied to the data sets with Figure 5(a) displaying the result from the Orpheus Island data and Figure 5(b) for the global data. The potential at the Orpheus site had mean value of 5W/m$^2$ and a maximum of over 50W/m$^2$ relating to a time when there was strong insolation and very low wind. Globally it can be seen that the effect of including the solar collector increased the average power output across the year by a factor of about 30 over those values from Figure 3(b). To give an indication of seasonal variability of this resource the model was run using the global data for a one month period in January and June, and the results are shown in Figure 6. The results show much larger power potentials available in local summer than winter.

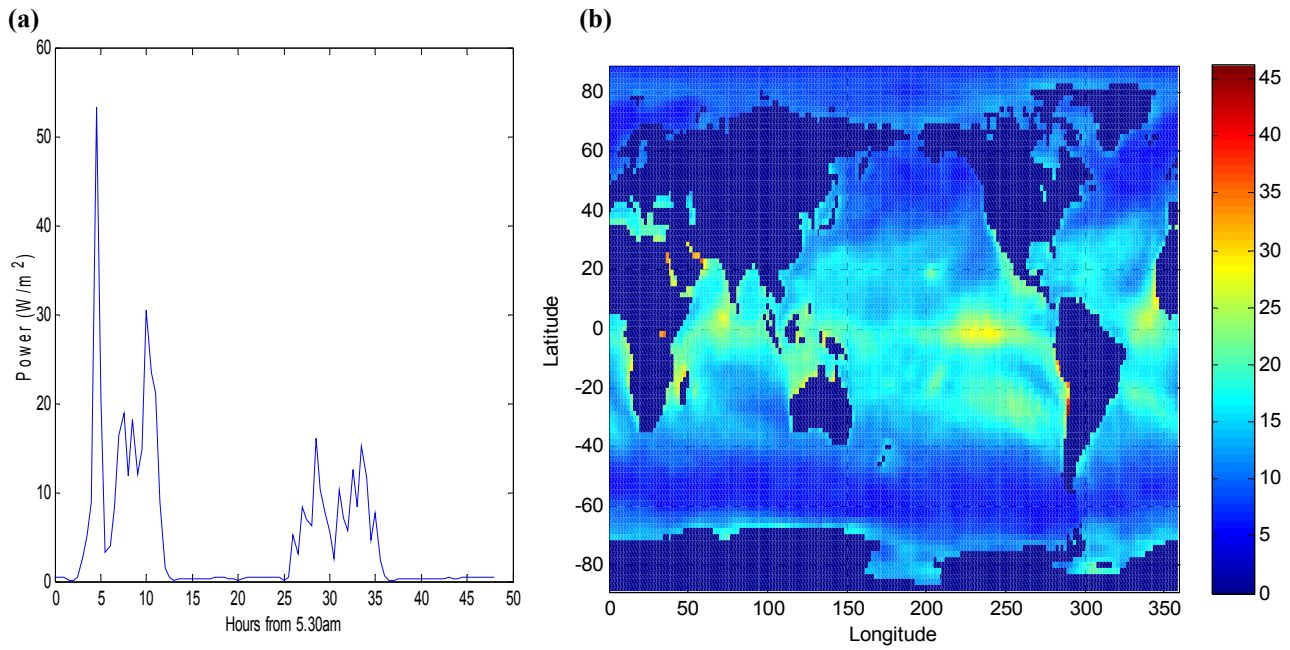


Figure 5: (a) Power output from Orpheus Island Site utilising the solar thermal harvesting model (b) Average power in $W/m^2$ for solar thermal method for 2008

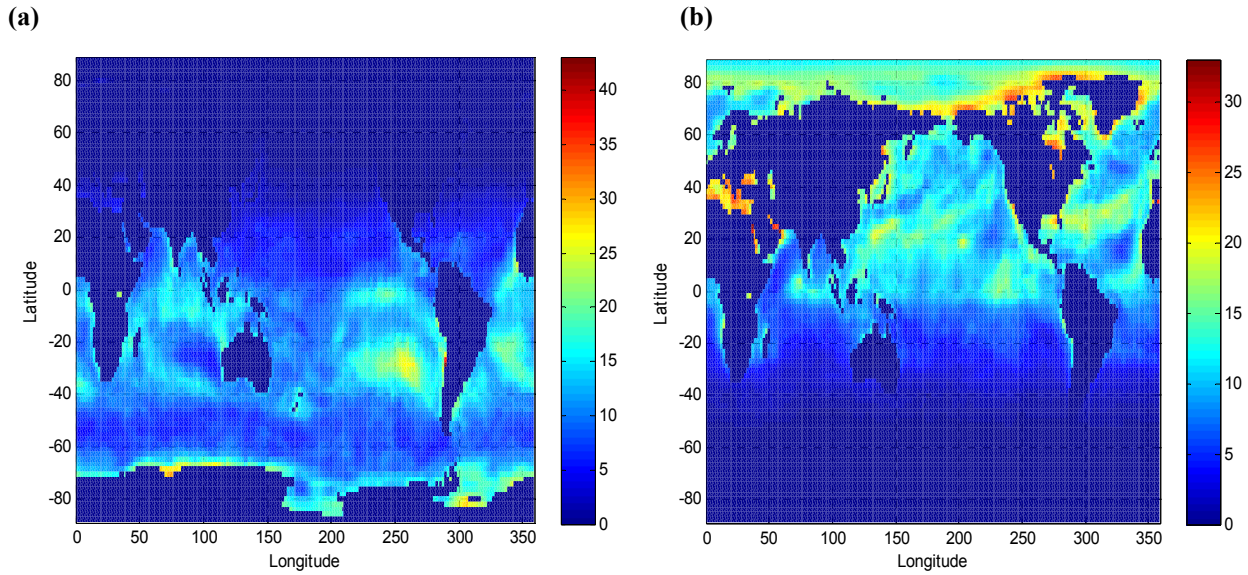


Figure 6: (a) Average power in $W/m^2$ for January 2008 (b) Average Power in $W/m^2$ for June 2008

## 4 DISCUSSION

The investigation into small scale renewable energy harvesting across the air/water interface performed here is basic, aimed as a first attempt to gauge the potential of this resource. The results have shown an expected average power in the order of $0.1W/m^2$ by utilizing the natural temperature gradient existing between the water and ambient air. By including a solar thermal collector the results of the models show the energy harvesting potential is increased substantially to

around $10W/m^2$. These results are intended to favour an upper limit to the power available from this resource stemming from the assumptions made and the use of the Carnot limit in calculating the conversion efficiencies.

Current TE devices achieve efficiencies in the order of 10% of Carnot so the results need to be scaled back by this amount to judge their effectiveness for powering wireless sensor nodes. The review in [1] reports that sensor nodes require in the order of 100mW of power in their active state. Therefore a thermal energy harvesting device operating across the air/water interface with/without a solar collector would need a cross-section around $0.1m^2$ and $10m^2$ respectively to ensure adequate energy provision to a wireless sensor node. On average however, a sensor node will need less power than this depending on its duty cycle as their sleep mode uses less than 1mW of power.

Clearly a $10m^2$ energy harvesting device is not appropriate for powering a wireless sensor node. Based on these results energy harvesting utilising the natural temperature gradient across the air/water interface is unsuitable for powering wireless sensor nodes. The results from the inclusion of a solar thermal collector showed a much greater potential with the result of an energy harvesting device with a $0.1m^2$ cross section able to power a sensor node. This sized device is possibly acceptable for aquatic based sensor node deployments thus thermal energy harvesting across the air/water interface utilising solar thermal energy may be a suitable candidate for powering aquatic based sensor nodes.

The results quoted need to be experimentally verified. The results from the solar thermal outputs have revealed that further effort for this energy harvesting technique is justified and as such experiments will be conducted to validate the results. This will allow findings to be used with confidence for further investigations.

The model needs to be extended to two dimensions to account for temperature gradients across the collector plate. Doing so would allow a better calculation of the optimum TE device area. Also the assumption that no temperature drop occurs between the TE device and the heat exchangers needs to be removed and this temperature drop accounted for. In their experimental investigation of similar devices Knight and Collins[7] showed that temperature differences up to 4% (5K) occurred, between the water temperature and the water side of the TE device, through the water side heat exchanger.

The use of glass or Perspex covers which are transparent to the incoming sunlight but opaque to the outgoing radiation is common practice in solar thermal engineering [6]. It has the effect of increasing the temperature of the collector plate by reducing the amount of outgoing radiation, $Q_r$, and reducing the amount of heat lost through convection, $Q_c$, by shielding the plate from the wind. This will increase the power output of the device. The use of such domes for the present application is a topic of current research and has been experimentally investigated in [7].

The data sets used were the polar opposite of each other. The Orpheus island data gave actual readings taken at one precise location every 30 minutes for 48 hours yielding a good indication of the power output available for one site at one time of the year for one set of environmental conditions. Had the data been taken from a different location, a different time of the year or if it had been a rainy day for example, the results may have been substantially different. The global data gave interpolated predicted readings as an average for a location over $10{,}000km^2$ every 6 hours for one year. While the results here give a good indication of the average outputs expected they have extremely poor time and spatial resolution reveal little about specific sites and actual outputs.

The data used was also biased to marine environments whereas aquatic wireless sensor node applications extend beyond this to include environments such as rivers, lakes, swamps, pools, drains and ponds. The potential of this resource in those environments may be quite different to those measured in the ocean and as such should be independently investigated with relevant data sets. Also the power outputs may be very site specific so this resource may prove to be an excellent power supply option in some areas and inadequate in others.

The results showed large fluctuations in the expected power outputs over many time scales. The power outputs from the Orpheus Island site show large fluctuations in response to the daily transitions of the Sun and globally the outputs showed large fluctuations in response to the changing seasons. For use with wireless sensor nodes this necessitates secondary energy storage to ensure a constant robust power supply. The duty cycles of these nodes/networks should possibly be aligned so that the tasks requiring high power are performed simultaneously to the times that the diurnal power fluctuations are at a maximum, and only perform essential and low power tasks when the harvested power is low. The daily times and magnitudes of these maxima/minima will likely change throughout the year so the duty cycles will either have to be adaptive and change through smart controls or be pre-programmed with a yearly cycle plan.

# 5 CONCLUSION

A model has been developed to estimate the power output of a thermal energy harvester to be used across an air/water interface. The model also incorporates the addition of a collector plate to improve the output by harvesting the local insolation. The model was applied to local and global data to estimate potential power output depending on location. The results showed that energy harvesting across the air/water interface is able to produce on the order of $10W/m^2$ on average across the globe throughout the year. The variability of this resource is very site and time dependant. Its potential for powering aquatic sensors seems viable and is the focus of further research.

## ACKNOWLEDGEMENTS

-NCEP Reanalysis data provided by the NOAA-CIRES Climate Diagnostics Center, Boulder, Colorado, USA, from their Web site at http://www.cdc.noaa.gov/.
-Thankyou to Pauline Mak and Dr Paola Petrelli from TPAC, University of Tasmania, Hobart, http://www.tpac.org.au/ for their support and assistance.
-Josh Davidson would also like to thank his PhD supervisor, Prof. Peter Ridd, for his valuable input.
-Thankyou to the CSIRO Energy Harvesting Team for their help and feedback.

## REFERENCES

[1] Knight, C., Davidson, J. and Behrens, S, "Energy Options for Wireless Sensor Nodes," Sensors, 8(12), 8037-8066 (2008).
[2] Lawrence, E.E. and Snyder, G.J., "A study of heat sink performance in air and soil for use in a thermoelectric energy harvesting device", IEEE Proceedings ICT '02, 21st International Conference on Thermoelectrics (2002)
[3] Stevens, J. "Optimal placement depth for air–ground heat transfer systems", Applied Thermal Engineering 24, (2004)
[4] Riffat and Ma, "Thermoelectrics: a review of present and potential applications", Applied Thermal Engineering, (2003)
[5] Takiishi et al, "Thermal Conductivity Measurements of Bismuth Telluride Thin Films by Using the 3 Omega Method", The 27th Japan Symposium on Thermophysical Properties, Kyoto,(2006)
[6] Duffie, J.A. and Beckman W.A., "Solar engineering of thermal processes", John Wiley & Sons, New York, (1980).
[7] Knight, C. and Collins, M., "Results of a water based thermoelectric harvesting device for powering wireless sensor nodes", Proc. SPIE 7288, (2009)